OPEN

Osthole inhibits the progression of human gallbladder cancer cells through JAK/STAT3 signal pathway both *in vitro* and *in vivo*

Tian Le Zou[a,b]*, Hong Fei Wang[b,c,]*, Tai Ren[b,c,]*, Zi Yu Shao[b,c], Rui Yan Yuan[b,c], Yuan Gao[b,c], Yi Jian Zhang[b,c], Xu An Wang[b,d] and Ying Bin Liu[b,d]

Osthole is an antitumor compound, which effect on Gallbladder cancer (GBC) has been not elucidated. This study focused on its anti-GBC effect and mechanism both *in vitro* and *in vivo*. The antiproliferation effect on cell lines NOZ and SGC-996 were measured by cell counting kit-8 (CCK-8) and colony formation assay. The effects on cell apoptosis and cell cycle were investigated by flow cytometry assay. The migration effect was checked by transwell assay and the expressions of proteins were examined by Western Blots. Also, we did an in-vivo experiment by intraperitoneal injection of osthole in nude mice. The results showed that cell proliferation and viability were inhibited in a dose- and time-dependent manner. The similar phenomenon was also found *in vivo*. Flow cytometric assay confirmed that osthole inhibited cells proliferation via inducing apoptosis and G2/M arrest. Transwell assay indicated that osthole inhibited the migration in a dose-dependent manner. Expression of key proteins related with apoptosis and cell cycle were testified after osthole treatment. Also, we found the key proteins involved in the JAK/STAT3 signal way decreased after osthole treatment. This study suggested that osthole can inhibit the progression of human GBC cell lines, thus maybe a potential drug for GBC treatment. *Anti-Cancer Drugs* 30:1022–1030 Copyright © 2019 The Author(s). Published by Wolters Kluwer Health, Inc.

Anti-Cancer Drugs 2019, **30:**1022–1030

Keywords: apoptosis, gallbladder cancer, JAK/STAT3 signaling pathway, migration, osthole, proliferation

[a]The Sixth Middle School of Guangzhou, Guangzhou, [b]Shanghai Key Laboratory of Biliary Tract Disease Research, [c]Laboratory of General Surgery and [d]Department of General Surgery, Xinhua Hospital Affiliated to Shanghai Jiaotong University, School of Medicine, Shanghai, China

Correspondence to Xu-An Wang, MD, Department of General Surgery, Xinhua Hospital, Shanghai Jiaotong University School of Medicine, No 1665 Kongjiang Road 200092, Shanghai, China
Tel/Fax: +86 21 25078813; email: wangxuan@xinhuamed.com.cn

*Dr Tian Le Zou, Dr Hong Fei Wang and Dr Tai Ren contributed equally to the writing of this article.

Received 12 March 2019 **Revised form accepted** 21 May 2019

Introduction

Gallbladder cancer (GBC) is the most common biliary tract cancer around the world [1]. Even the GBC at early stage may have a poor prognosis [2]. No effective therapy has been found in patients with advanced GBC. The five-year survival rate of GBC is less than 16% [3]. New therapy for GBC is demanded.

An increasing number of research suggest that some natural agents may have antitumor properties and maybe have potential treatment effect [4]. Osthole is a natural compound derived mainly from fruits of *Fructus cnidii*. It has been used in the treatment in colitis, bone fracture, asthma and brain injury [5–8]. Recent studies showed that osthole could suppress cancer cell viability, proliferation and migration ability via apoptosis, cell cycle arrest and inhibiting epithelial–mesenchymal transition (EMT) [9–12]. However, the effect of osthole on GBC has not been studied. Therefore, this study was designed to explore the function of osthole on GBC cell lines (NOZ and SGC-996) both *in vivo* and *in vitro* and its potential mechanism.

Materials and methods

Cell lines and culture

The human GBC cell lines NOZ and SGC-996 were both purchased from Shanghai Institute Biological Science, Chinese Academy of Science (Shanghai, China). NOZ cells were cultured in William's medium (Gibco, New York, USA) and SGC-996 cell line was cultured in Rosewell Park Memorial Institute 1640 (RPMI-1640) (Gibco). Both of the above media were supplemented with 10% fetal bovine serum (Gibco), 100 µg/ml streptomycin, and 100 U/ml penicillin (Hyclone, Logan, Uttah, USA). The two cell lines were maintained at 37°C in a humidified atmosphere with 5% CO_2.

Cell viability assay

The effect of osthole on cell viability was measured by cell counting kit-8 (CCK-8) assay. The NOZ and

0959-4973 Copyright © 2019 The Author(s). Published by Wolters Kluwer Health, Inc. DOI: 10.1097/CAD.0000000000000812

SGC-996 cell lines (4×10^3/well) were seeded on 96-well plate. After overnight incubation, the cells were treated with different concentration (0, 50, 100, 150, and 200 μM) of osthole for 24, 48, and 72 hours. After the treatment, 100 μl 10% CCK-8 solution was added into the 96-well plate. The absorbance of the solution was detected at 450nm with a microplate reader (Quant Bio Tek Instruments, Winooski, Vermont, USA) after an incubation of 2.5 hours.

Colony formation assay

The NOZ and SGC-996 cell lines in the logarithmic growth phase were digested and resuspended. Then 500 cells were seeded into each well of 6-well plates (Corning, Corning, New York, USA). After incubated overnight, the cells were treated with osthole (0, 50, 100, and 150 μM) for 48 hours. Then all the Osthole-contained media were removed and replaced with fresh medium every second day till to 14 days when the colony formed. Then cells were fixed with 4% paraformaldehyde for 15 minutes and stained with 0.1% crystal violet (Sigma-Aldrich) for 15 minutes. After washed with PBS, the plates were air dried, and stained colonies were photographed using a microscope (Leica, Wetzlar, Germany). The total number of colonies (>50 cells/colony) was counted manually.

Cell apoptosis assay

The annexin V/propidium iodide assay was performed according to the manufacturer's instructions (Invitrogen, Carlsbad, California, USA) to analyze apoptosis. NOZ and SGC-996 cell lines were seeded into 6-well plates (Corning) with 1×10^6 cells per well and treated with osthole (0, 50, 100, and 150 μM). After incubated for 48 hours, the cells were collected and washed twice with cold PBS, then centrifuged and resuspended at a density of 1×10^6 cells/ml into 100 μl of binding buffer containing 5 μl of Annexin V-FITC and 5 μl of PI working solution (100 μg/ml). After incubated at room temperature for 15 minutes in the dark, 100 μl of binding buffer was added to each sample. The stained cells were analyzed by flow cytometry (BD, San Diego, California, USA) for at least 10 000 events. Cells populations in different quadrants were measured by quadrant statistics.

Cell cycle analysis

The NOZ and SGC-996 cells were seeded into a 6-well culture plate, then treated with different concentrations of osthole (0, 50, 100, and 150 μM for both strains of cells) for 24 hours. Both floating and adherent cells were collected and washed twice with PBS. After fixed in cold 70% ethanol at 4°C overnight, the cells were incubated with 10 mg/ml RNase and 1 mg/ml propidium iodide (Sigma-Aldrich, St.Louis, Missouri, USA) at room temperature for 30 minutes in the dark. The samples were analyzed with a flow cytometer (BD Biosciences, San Diego, California, USA), and the percentage of cells in the G0/G1, S and G2/M phases were determined using Cell Quest acquisition software (BD Biosciences).

Cell invasion assay

Cell migration was performed using 8-μm transwell filters in 24-well plates (BD Biosciences, Franklin Lakes, New Jersey, USA). NOZ and SGC-996 (2×10^4/cells) were plated in the upper chamber, in 200 μl of serum-free medium. Five-hundred microliters of medium supplemented with 10% fetal bovine serum (FBS) was subsequently added to the lower chamber. The cells were subsequently allowed to incubate for 22 (SGC-996) and 14 hours (NOZ), and then the cells would migrate to the lower compartment and thus adhered to the lower membrane. Then, the cells were fixed with methanol and stained with crystal violet. The cells in three randomly selected fields in each well were counted and photographed. The above experiments were performed three times.

Western blot assay

The Western blot analysis was conducted as described in [13]. The total protein was extracted from the cells using lysis buffer (Beyotime, China) and protease inhibitor (Biocolors, China). Lysis buffer and protease inhibitor were used after mixed in proportion of 1:100. Equal amounts of protein were loaded on a 10 or 13% SDS-PAGE gel. The lysates were resolved by electrophoresis (80 V for 30 minutes and 120 V for 1.0 or 1.5 hours) and transferred onto NC membranes (nitrocellulose membrane, Bio-Rad, Hercules, California, USA). After blocking in 5% nonfat milk for 2 hours at room temperature, the membranes were incubated with cleaved-PARP, cleaved-caspase 3, Bax, Bcl-2,Cyclin D1, cyclin B, CDK1, cdc25A, vimentin, E-cadherin, N-cadherin and Snail (1:1000, Cell Signaling Technology, Danvers, Massachusetts, USA) and then incubated with a horseradish peroxidase-conjugated goat antirabbit/antimouse secondary antibody (1:5000; Abcam, Cambridge, United Kingdom). β-actin was used as an internal control to ensure equal protein loading.

Tumorigenicity assay in nude mice

Four-to-six-week male BALB/c nude immune deficiency mice were brought from the Shanghai SLAC Laboratory Animal Co., Ltd. (Shanghai, China) and housed under specific pathogen-free condition. All animal experimental procedures were approved by the Institutional Animal Care and Use Committee of Shanghai Jiao Tong University (Shanghai, China). NOZ cells (10×10^5/ml) were resuspended into single cell condition in 100 μl fresh medium and were injected subcutaneously into the left axilla of each nude mice. After 5 days injection, mice were randomly divided into three groups and were intraperitoneally injected with osthole (fresh medium for control group, and 10 and 30 mg/kg for treatment groups) every second day. All mice were mercy sacrificed and the tumor were collected and measured after 28 days.

Statistical analysis

Statistical analyses were conducted using SPSS 19.0 software. All data points represent the mean of triplicate independently data points, and all quantified data are expressed as the mean ± SD. Statistical significance was calculated using the Student's *t*-test, and *P* values of less than 0.05 (**P* < 0.05, ***P* < 0.01, ****P* < 0.001) were considered statistically significant.

Results

Osthole inhibited the proliferation of NOZ and SGC-996 cell lines

To evaluate the effect of osthole on cell proliferation, GBC cell lines NOZ and SGC-996 were treated with different concentrations (0, 50, 100, 150, and 200 μM) of osthole for 24, 48, and 72 hours. Cell proliferation was measured by CCK-8 and colony formation assays.

Fig. 1

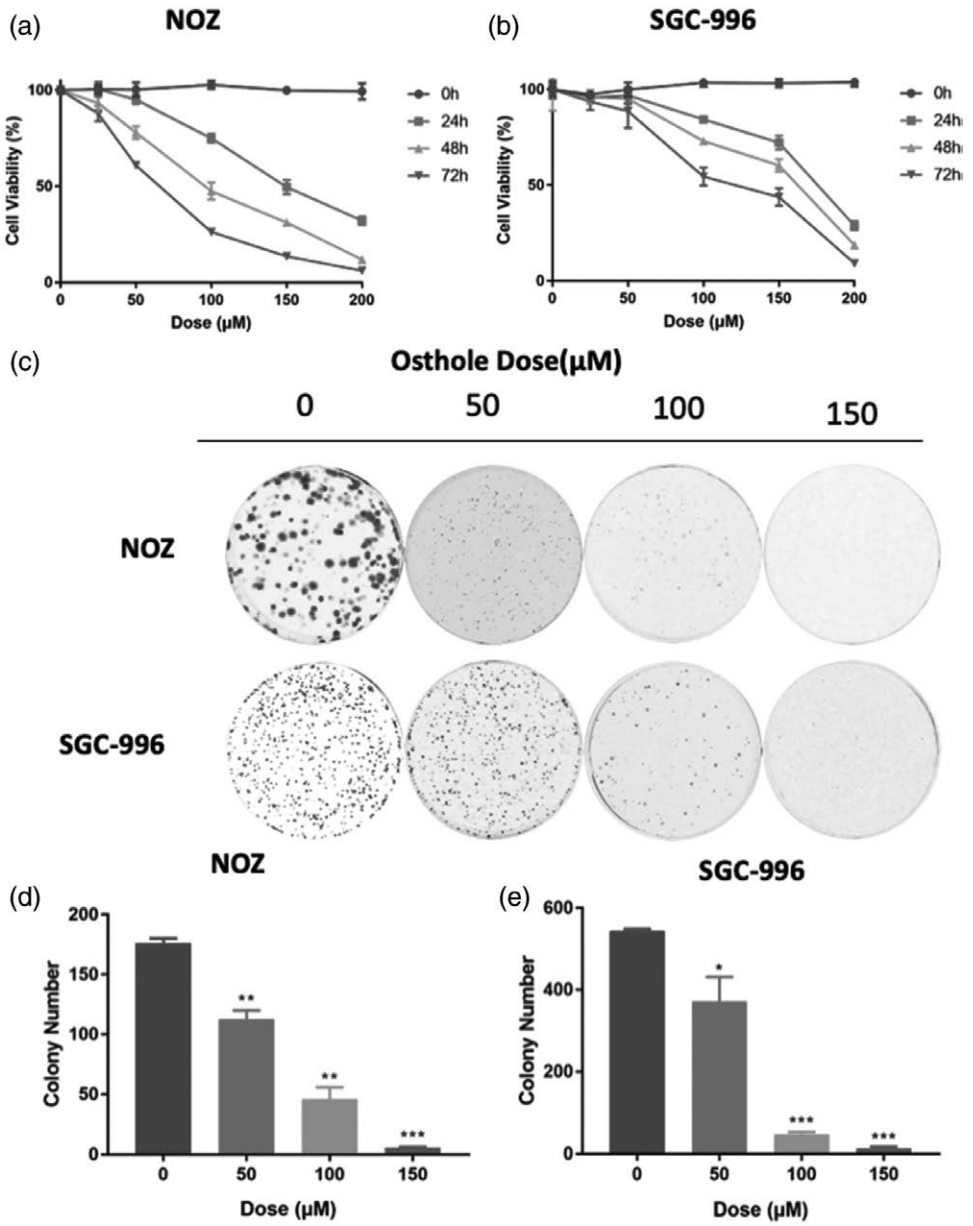

The chemical structure of osthole. Osthole inhibits the proliferation and colony formation of GBC cells. (a) and (b) NOZ and SGC-996 cells were treated with osthole (0, 50, 100, 150, and 200 μM) for 24, 48, and 72 hours. Cell viability was determined by CCK-8 assays. (c) Cells were treated with different concentrations of osthole and cultured in fresh medium for 14 days to form colonies. (d) and (e) Detailed information on colony formation are shown. Data are presented as mean ± SD (***n***=3). **P*<0.05, ***P*<0.01, ****P*<0.001. GBC, gallbladder cancer.

Both assays demonstrated that osthole inhibited the viability of GBC cell lines in a time- and dose-dependent manner (Fig. 1a–c). Furthermore, the colony count confirmed this result (Fig. 1d, e). All these results revealed that osthole has antiproliferation effect on GBC *in vitro*.

Osthole promoted the apoptosis of NOZ and SGC-996 cell lines

To reveal the mechanism of cell viability inhibition mediated by osthole, cell apoptosis was detected by Annexin V and propidium iodide staining. The results indicated that Osthole induced both NOZ and SGC-996 cell apoptosis in a dose-dependent manner (Fig. 2a), the percentage of early apoptosis cells increased significantly after treatment with Osthole for 48 hours. When compared with the control group, the percentage of early apoptotic cells in NOZ and SGC-996 populations treated with 50 μM of Osthole were increased from 2.70% ± 0.42% to 54.1% ± 5.09% and 3.40% ± 0.71% to 52.05% ± 5.16%, respectively ($P < 0.05$) (Fig. 2b, c).

To further confirm that osthole induced cell apoptosis in human GBC cell lines, the expression of proapoptosis and antiapoptosis proteins such as Bcl-2 family and caspase family proteins were detected by Western blot assay. Our results revealed that osthole significantly increased the expression of proapoptosis proteins including cleaved-caspase3; cleaved-PARP and Bax, while the expression of antiapoptosis protein Bcl-2 was decreased (Fig. 2d).

Osthole induced G2/M cell cycle arrest of NOZ and SGC-996 cell lines

To further explore the potential mechanism, cell cycle was analyzed. As observed in Fig. 3a–c, the increasing proportion of cells in the G2/M phase after treatment with osthole for 24 hours indicated G2/M phase cell cycle arrest, and the effect was enhanced with a higher concentration of osthole.

The expression of cell cycle regulatory proteins was examined. The Western blot assay showed that the proteins associating with G2/M phase including cyclin D1, cyclin B, CDK1 and cdc25A were decreased (Fig. 3d), in accordance with the cell cycle assay. Thus, osthole could induce G2/M phase arrest through downregulation of the cell cycle proteins.

Osthole inhibited the invasion of NOZ and SGC-996 cell lines

As early metastasis is the main reason that attributed to the poor prognosis of GBC patients, the function of osthole on GBC cell migration and invasion was detected by cell invasion assay. As shown in Figure 4a, osthole significantly reduced the number of migrated cells compared with the control group in a dose-dependent manner. The number of invaded cells was reduced by 25% and by 87.5% after treatment with 50 and 150 μM osthole for 48 hours in NOZ cell line as compared with the control group (Fig. 4b, c). The similar result was confirmed in SGC-996 cell line.

Vimentin, E-cadherin, N-cadherin, and Snail are proteins known as degrading extracellular matrix components and promoting tumor cellular invasion. These proteins were analyzed by Western blot assay after treatment with different concentration of osthole for 48 hours in both NOZ and SGC-996 cell lines, the result showed that expression of Vimentin, N-cadherin, and Snail was significantly decreased and E-cadherin increased in a dose-dependent manner (Fig. 4d).

Osthole inhibited the progression of human GBC cells through JAK/STAT3 signal pathway

JAK/STAT3 signal pathway plays an important role in cell proliferation, cell survival, and tumor metastasis. In order to verify whether osthole could inhibit GBC cell via JAK/STAT3 signal pathway, we conducted Western blot assay to test the critical proteins included in JAK/STAT3 signal pathway. After incubating with osthole, the expression of protein JAK, p-JAK, ATAT3, and p-STAT3 were all decreased in NOZ and SGC cells, as shown in Figure 5. Those data revealed that osthole may play its inhibitory effect through JAK/STAT3 signal pathway.

Osthole inhibited the growth of NOZ xenografts in nude mice

Our previous data confirmed that osthole had an antitumor effect on GBC *in vitro*. To further assess its tumor suppression ability of osthole *in vivo*, the tumorigenicity of NOZ cells in nude mice was studied. The vehicle (William's medium) or osthole (10 and 30 mg/kg daily by intraperitoneal injection) was used to the nude mice bearing NOZ cell xenografts for 28 days. As shown in Figure 6a–c, both tumor size and weight were decreased in a dose-dependent manner after treatment with osthole. Besides, the body weight among the three groups of mice was no significant difference, indicating no systemic toxicity of osthole treatment.

Discussion

Osthole is a natural compound that is extracted from the fruit of the *F. cnidii* plant. The formula of osthole is C15H16O3 and it has a wide range of biological functions, such as anticonvulsant [7], antiinflammatory [14], and prevention of osteoporosis [11]. It has also been reported that osthole could inhibit the growth of cancer cells by inducing apoptosis or arresting the cell cycle, as well as inhibit tumor migration through the EMT pathway [9]. However, there has been no report whether osthole has effects on GBC, which is an extremely malignant tumor with poor prognosis.

In our study, we first conducted CCK-8 and colony formation assay to evaluate the antiproliferation effect of osthole on human GBC cell lines NOZ and SGC-996.

Fig. 2

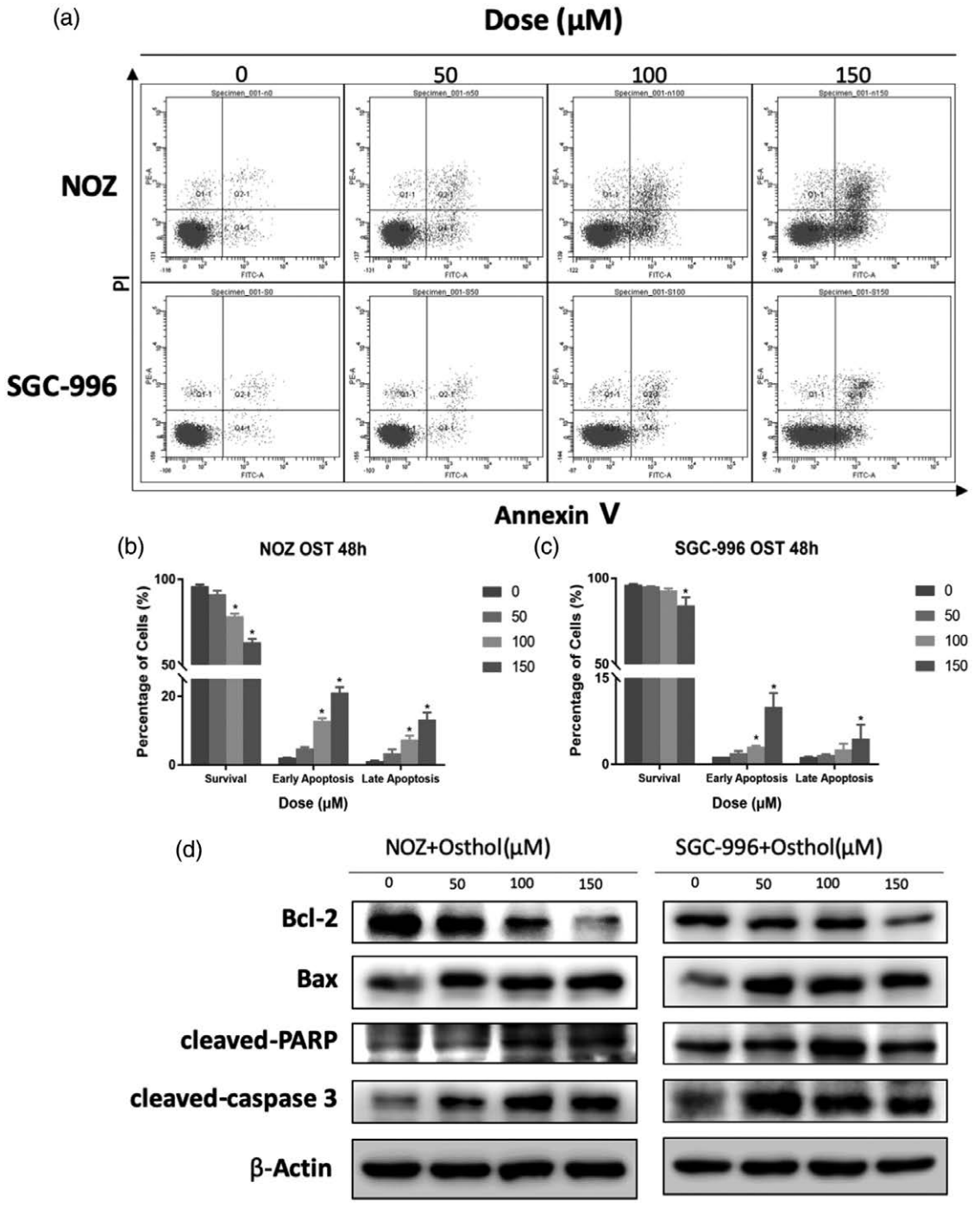

Osthole induces apoptosis in GBC cells. (a) NOZ and SGC-996 cells were incubated with cordycepin (0, 50, 100, and 150 μM) for 48 hours, then stained with Annexin V/propidium iodide and analyzed by flow cytometry. The Q3 quadrant (Annexin-V−/propidium iodide−), Q4 quadrant (Annexin-V+/propidium iodide−), and Q2 quadrant (Annexin-V+/propidium iodide+) represent the group of normal cells, early apoptosis, and late apoptosis, respectively. (b) and (c) The percentage of cells in each stage is presented. Data are presented as mean ± SD ($n=3$). *$P<0.05$, **$P<0.01$, ***$P<0.001$. (d) Representative results of Western blot analysis for the protein level of cleaved caspase-3, cleaved PARP, Bcl-2, and Bax in GBC cells treated with osthole at indicated doses for 48 hours. β-actin was used as a loading control. GBC, gallbladder cancer.

Fig. 3

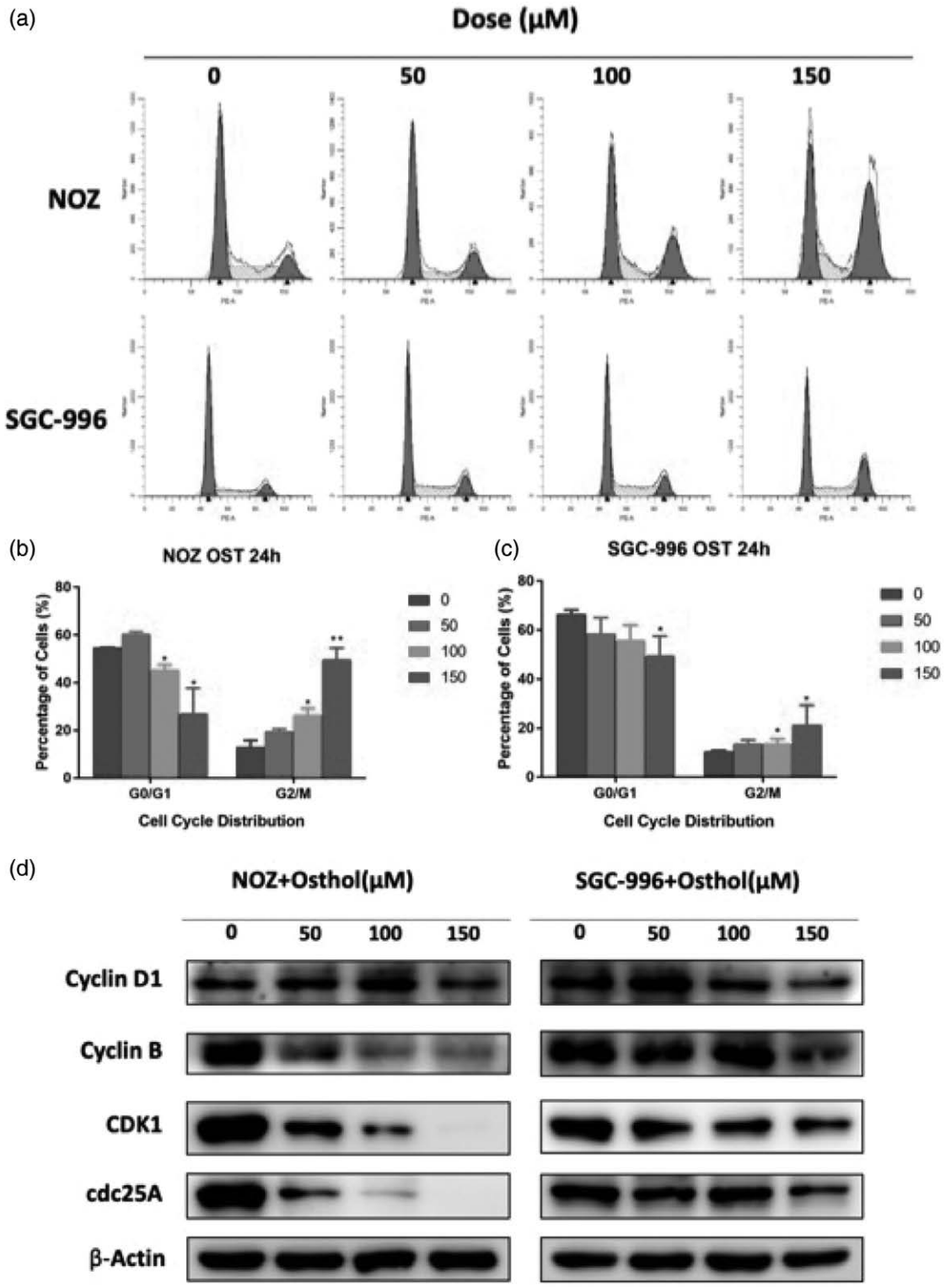

Osthole induces G2/M phase cell cycle arrest and regulates the expression of cell cycle-related proteins in GBC cells. NOZ and SGC-996 cells were treated with osthole (0,50,100, and 150 μM) for 24 h. (a) The cell cycle phases of the treated cells were evaluated by flow cytometry. (b) and (c) Data were expressed as mean ± SD (***n***=3). Results are representative of 3 independent experiments. **P*<0.05, ***P*<0.01 versus. the control group. (d) The expression levels of cyclin D1, cyclin B, CDK1 and cdc25A were measured by Western Blot analysis, and β-actin was used as a loading control. GBC, gallbladder cancer.

Fig. 4

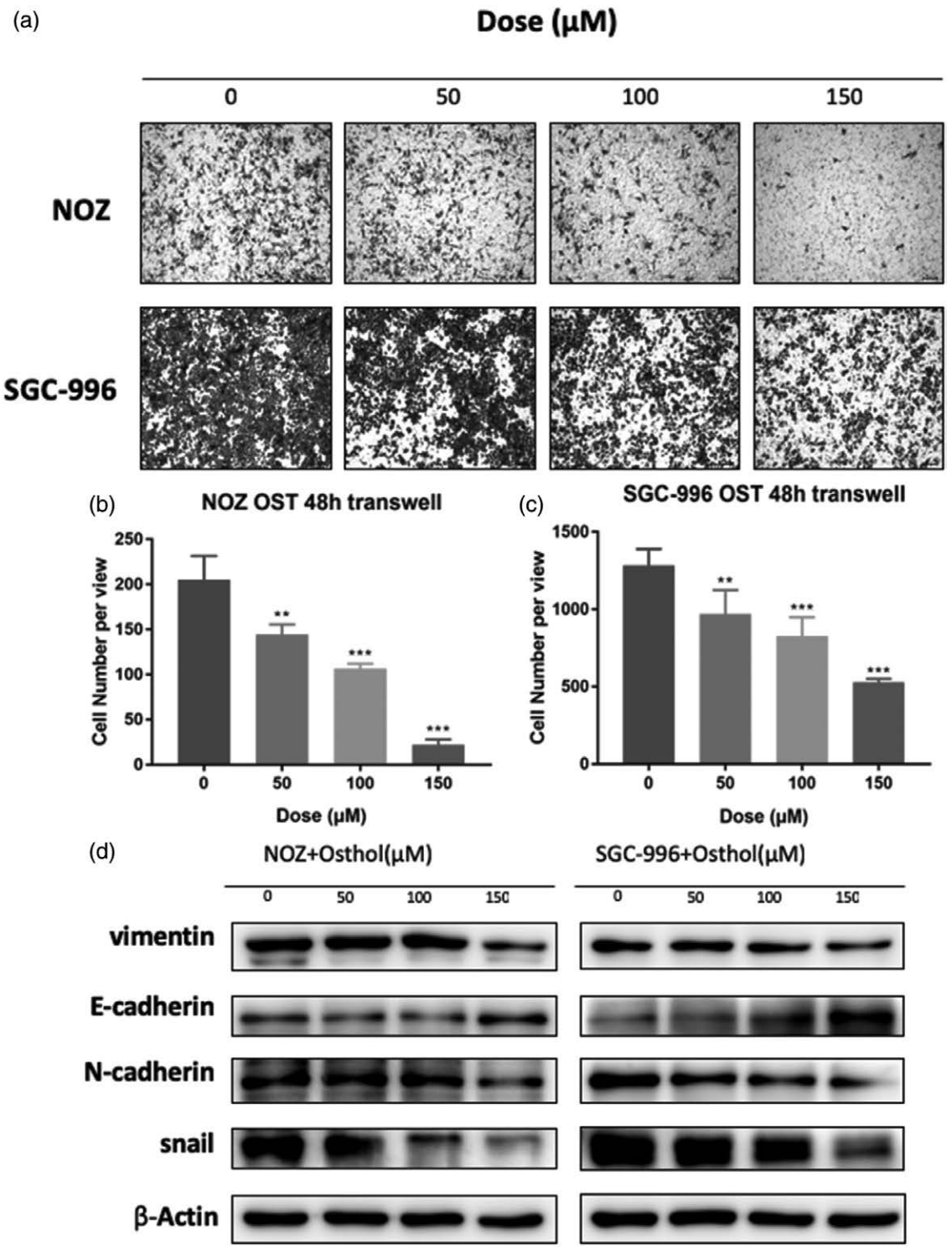

Effect of osthole on the invasive potency of human GBC NOZ and SGC996 cells. (a) Cells were treated with osthole (0, 50,100, and 150 μM) for 48 hours for invasion assay. (b) and (c) Cell invasion numbers were counted. *$P<0.05$, **$P<0.01$, ***$P<0.001$. (d) The protein expression of vimentin, E-cadherin, E-cadherin, and Snail was detected by Western Blot after treatment for 48 hours. GBC, gallbladder cancer.

Fig. 5

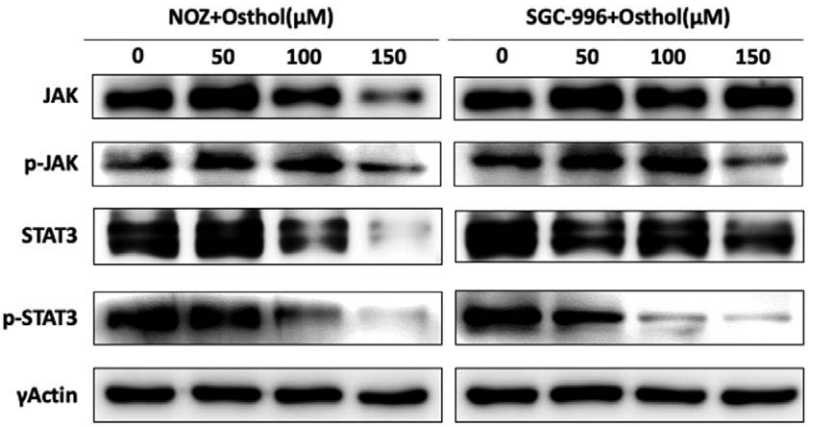

The expression of proteins correlated with JAK/STAT3 signaling pathway. JAK, p-JAK, ATAT3, and p-STAT3 were all decreased in NOZ and SGC-996 cells after treated with osthole (0, 50,100, and 150 μM) for 48 hours.

Fig. 6

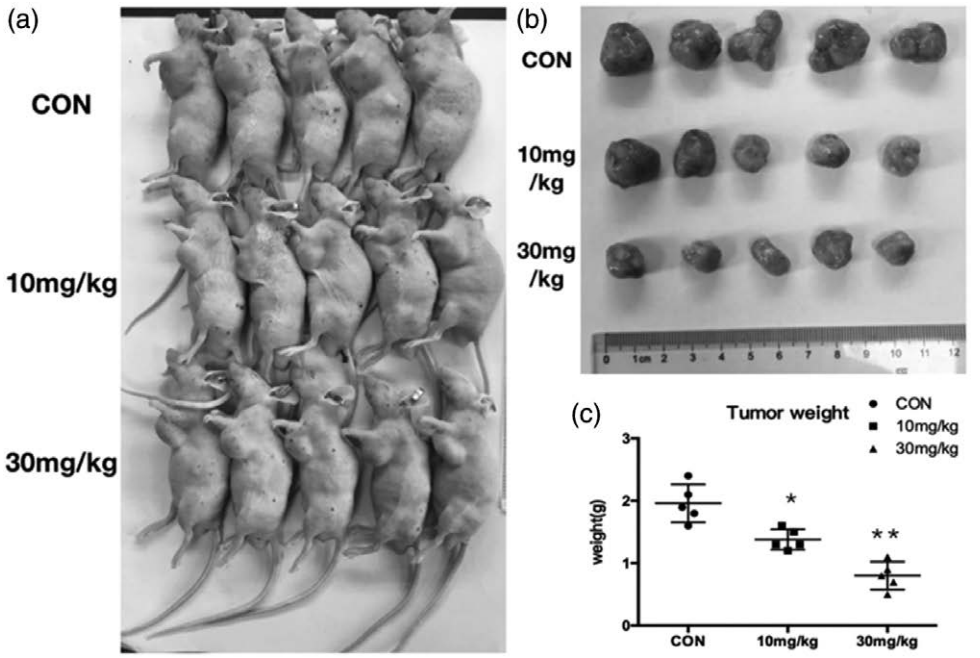

Osthole inhibits the proliferation of GBC NOZ cells in vivo. (a) Photographs of tumor xenografts 28 days after inoculation. (b) and (c) Tumor size and weight in the osthole group at the end of the experiment was significantly lower than that in the control group. Data are presented as mean ± SD (n=3). *P<0.05, **P<0.01. GBC, gallbladder cancer.

The results showed that osthole had a significant inhibitory effect on the proliferation of NOZ and SGC-996 cells in a dose- and time-dependent manner. Also, we found similar results on the subcutaneous tumor animal model. Then, we used different concentrations of osthole (0, 50, 100, and 150 μM) to examined its influence on the apoptosis of GBC cells and found that the apoptosis of NOZ and SGC-996 cells were significantly enhanced, and the degree of apoptosis was increased as the concentration of osthole increasing. Western Blot results showed that the ratio of Bcl-2/Bax was evidently lower than the control group, and the expression of cleaved-PARP, cleaved-caspase3 in NOZ and SGC-996 were also decreased. This result confirmed that osthole promotes apoptosis of NOZ and SGC-996 cells. Because apoptosis is an important mechanism affecting cell proliferation [13], we speculate

that osthole can reduce GBC cell proliferation by inducing apoptosis-related proteins.

The change of cell cycle is another mechanism that affects the proliferation of living cells. We also selected the propidium iodide single staining flow cytometry assay to explore the change in cell cycle. After treating with osthole, the G2/M phase cell of NOZ and SCG-996 were both increased, which indicated that osthole induced cell cycle arrest. Western blot results showed that the expression levels of Cyclin D1, Cyclin B, CDK1, and cdc25A proteins in NOZ and SGC-996 cells were decreased, which were related to the G2/M phase cell cycle. Therefore, we speculated that osthole inhibited the proliferation of NOZ and SGC-996 cells by G2/M phase cell cycle arrested.

EMT is one of main mechanism associated with cancer development, especially metastasis. The ratio of E-cadherin and N-cadherin is an indicator of EMT degree. The cell invasion assay showed that the invasion ability of GBC cells was significantly decreased after treated with osthole. Western blot results showed that the expression of vimentin, N-cadherin, and snail decreased, and the expression of E-cadherin increased. The increasing ratio of E-cadherin to N-cadherin confirmed that osthole inhibited the invasion of human GBC cells.

In addition, typical signal pathways were examined to reveal the possible mechanism of osthole on human GBC cells. Through Western blot assay, p-JAK and p-STAT3 proteins in the pathway were most markedly altered in osthole-treated GBC cells. p-JAK and p-STAT3 are the key proteins of JAK/STAT3 signaling pathway, which is an important signal transduction pathway in cells and plays an important role in cell growth, survival, proliferation, apoptosis, and angiogenesis [15]. Abnormal activation of JAK/STAT3 signal pathway is associated with progression of cancer. In our study, we found that osthole inhibited the proliferation and invasion of GBC cells by suppressing the JAK/STAT3 signaling pathway.

Conclusion

GBC is a common bile duct malignancy with extremely bad behavior and lack of effective treatment. In the current study, our data indicated that osthole extracted from natural plants have potential anti-GBC activities *in vitro* and *in vivo* through inhibition of cell proliferation, promotion of apoptosis, and induction of cell cycle arrest. Osthole is also correlated with JAK/STAT3 signaling pathway. Taken together, all these results provide a solid experimental basis for the potential treatment use of osthole on GBC, but further clinical studies are needed.

Acknowledgements

This study was supported by the Shanghai Natural Science Foundation (No 17ZR1418500), and Shanghai Pujiang Program (No 17PJD025).

Conflicts of interest

There are no conflicts of interest.

References

1 Torre LA, Siegel RL, Islami F, Bray F, Jemal A. Worldwide burden of and trends in mortality from gallbladder and other biliary tract cancers. *Clin Gastroenterol Hepatol* 2018; **16**:427–437.
2 Wang XA, Xiang SS, Li HF, Wu XS, Li ML, Shu YJ, *et al*. Cordycepin induces S phase arrest and apoptosis in human gallbladder cancer cells. *Molecules* 2014; **19**:11350–11365.
3 Swaminathan R, Lucas E, Sankaranarayanan R. Cancer survival in Africa, Asia, the Caribbean and Central America: database and attributes. *Iarc Sci Publ* 2011; **162**:257–291.
4 Mignani S, Rodrigues J, Tomas H, Zablocka M, Shi X, Caminade AM, Majoral JP. Dendrimers in combination with natural products and analogues as anti-cancer agents. *Chem Soc Rev* 2018; **47**:514–532.
5 Khairy H, Saleh H, Badr AM, Marie MS. Therapeutic efficacy of osthole against dinitrobenzene sulphonic acid induced-colitis in rats. *Biomed Pharmacother* 2018; **100**:42–51.
6 Wang P, Ying J, Luo C, Jin X, Zhang S, Xu T, *et al*. Osthole promotes bone fracture healing through activation of BMP signaling in chondrocytes. *Int J Biol Sci* 2017; **13**:996–1007.
7 Chiang CY, Lee CC, Fan CK, Huang HM, Chiang BL, Lee YL. Osthole treatment ameliorates Th2-mediated allergic asthma and exerts immunomodulatory effects on dendritic cell maturation and function. *Cell Mol Immunol* 2017; **14**:935–947.
8 Yan Y, Kong L, Xia Y, Liang W, Wang L, Song J, *et al*. Osthole promotes endogenous neural stem cell proliferation and improved neurological function through notch signaling pathway in mice acute mechanical brain injury. *Brain Behav Immun* 2018; **67**:118–129.
9 Feng H, Lu JJ, Wang Y, Pei L, Chen X. Osthole inhibited TGF β-induced epithelial-mesenchymal transition (EMT) by suppressing NF-κb mediated snail activation in lung cancer A549 cells. *Cell Adh Migr* 2017; **11**:464–475.
10 Wang L, Yang L, Lu Y, Chen Y, Liu T, Peng Y, *et al*. Osthole induces cell cycle arrest and inhibits migration and invasion via PTEN/Akt pathways in osteosarcoma. *Cell Physiol Biochem* 2016; **38**:2173–2182.
11 Shokoohinia Y, Jafari F, Mohammadi Z, Bazvandi L, Hosseinzadeh L, Chow N, *et al*. Potential anticancer properties of osthol: a comprehensive mechanistic review. *Nutrients* 2018; **10**:36.
12 Qi XK, Han HQ, Zhang HJ, Xu M, Li L, Chen L, *et al*. OVOL2 links stemness and metastasis via fine-tuning epithelial-mesenchymal transition in nasopharyngeal carcinoma. *Theranostics* 2018; **8**:2202–2216.
13 Zhang Y, Zhang XX, Yuan RY, Ren T, Shao ZY, Wang HF, *et al*. Cordycepin induces apoptosis in human pancreatic cancer cells via the mitochondrial-mediated intrinsic pathway and suppresses tumor growth in vivo. *Onco Targets Ther* 2018; **11**:4479–4490.
14 Jiang G, Liu J, Ren B, Tang Y, Owusu L, Li M, *et al*. Anti-tumor effects of osthole on ovarian cancer cells in vitro. *J Ethnopharmacol* 2016; **193**:368–376.
15 Huynh J, Etemadi N, Hollande F, Ernst M, Buchert M. The JAK/STAT3 axis: a comprehensive drug target for solid malignancies. *Semin Cancer Biol* 2017; **45**:13–22.